

# ApoE<sup>-/-</sup>Fas<sup>-/-</sup> C57BL/6 mice: a novel murine model simultaneously exhibits lupus nephritis, atherosclerosis, and osteopenia

Xuebing Feng,<sup>1,\*</sup> Hongyun Li,<sup>\*</sup> Alexis A. Rumbin,<sup>\*</sup> Xuping Wang,<sup>†</sup> Antonio La Cava,<sup>\*</sup> Katherine Brechtelsbauer,<sup>\*</sup> Lawrence W. Castellani,<sup>†</sup> Joseph L. Witztum,<sup>§</sup> Aldons J. Lulis,<sup>†</sup> and Betty P. Tsao<sup>2,\*</sup>

Division of Rheumatology, Department of Medicine,<sup>\*</sup> University of California, Los Angeles, CA; Departments of Microbiology, Immunology, and Molecular Genetics, Medicine, and Human Genetics and the Molecular Biology Institute,<sup>†</sup> University of California, Los Angeles, CA; and Department of Medicine,<sup>§</sup> University of California San Diego, La Jolla, CA

**Abstract** To establish a mouse model of accelerated atherosclerosis in lupus, we generated apolipoprotein E-deficient (apoE<sup>-/-</sup>) and Fas<sup>lpr/lpr</sup> (Fas<sup>-/-</sup>) C57BL/6 mice. On a normal chow diet, 5 month old apoE<sup>-/-</sup>Fas<sup>-/-</sup> mice had enlarged glomerular tuft areas, severe proteinuria, increased circulating autoantibody levels, and increased apoptotic cells in renal and vascular lesions compared with either single knockout mice. Also, double knockout mice developed increased atherosclerotic lesions but decreased serum levels of total and non-HDL cholesterol compared with apoE<sup>-/-</sup>Fas<sup>+/+</sup> littermates. Moreover, female apoE<sup>-/-</sup>Fas<sup>-/-</sup> mice had lower vertebral bone mineral density (BMD) and bone volume density (BV/TV) than age-matched female apoE<sup>-/-</sup>Fas<sup>+/+</sup> mice. Compared with apoE<sup>-/-</sup>Fas<sup>+/+</sup> and apoE<sup>+/+</sup>Fas<sup>-/-</sup> mice, apoE<sup>-/-</sup>Fas<sup>-/-</sup> mice had decreased circulating oxidized phospholipid (OxPL) content on apoB-100 containing lipoprotein particles and increased serum IgG antibodies to OxPL, which were significantly correlated with aortic lesion areas ( $r = 0.58$ ), glomerular tuft areas ( $r = 0.87$ ), BMD ( $r = -0.57$ ), and BV/TV ( $r = -0.72$ ). These results suggest that the apoE<sup>-/-</sup>Fas<sup>-/-</sup> mouse model might be used to study atherosclerosis and osteopenia in lupus. Correlations of IgG anti-OxPL with lupus-like disease, atherosclerosis, and bone loss suggested a shared pathway of these disease processes.—Feng, X., H. Li, A. A. Rumbin, X. Wang, A. La Cava, K. Brechtelsbauer, L. W. Castellani, J. L. Witztum, A. J. Lulis, and B. P. Tsao. ApoE<sup>-/-</sup>Fas<sup>-/-</sup> C57BL/6 mice: a novel murine model simultaneously exhibits lupus nephritis, atherosclerosis, and osteopenia. *J. Lipid Res.* 2007. 48: 794–805.

**Supplementary key words** oxidized phospholipid • apoptosis • autoantibodies

Cardiovascular complications related to atherosclerosis are common among patients with systemic lupus erythematosus (SLE) and contribute to their disability and death (1–4). Women with SLE between 35 and 44 years old have an estimated 50-fold increased risk of myocardial infarction compared with age- and gender-matched controls (5). After controlling for traditional Framingham risk factors, the relative risk for early coronary heart disease attributed to SLE itself is 7.5-fold (6). An increased prevalence of subclinical atherosclerosis in SLE has also been established: 37% of SLE patients versus 15% of controls have plaques detectable by carotid artery ultrasound (3), and 31% of SLE patients versus 9% of controls exhibit coronary artery calcification (4). The disease processes of SLE itself, including a longer duration of disease, a higher damage-index score, and less aggressive immunosuppressive therapy, are independent risk factors for atherosclerosis (3).

Similar to accelerated atherosclerosis in SLE, bone loss in SLE involves both traditional osteoporosis risk factors and lupus-related factors. More than one-third of SLE patients were osteopenic by bone mineral density (BMD) scanning (7, 8) More strikingly, at least 20% of SLE patients (mean age of 41 years) had osteoporotic vertebral

Abbreviations: apoE, apolipoprotein E; B6, C57BL/6; BMD, bone mineral density; BV/TV, bone volume density; dsDNA, double-stranded DNA; OxLDL, oxidized low-density lipoprotein; OxPL, oxidized phospholipid; PGPc, 1-palmitoyl-2-glutaroyl-*sn*-glycero-3-phosphorylcholine; POVPC, 1-palmitoyl-2(5-oxovaleroyl)-*sn*-glycero-3-phosphorylcholine; RLU, relative light units; SLE, systemic lupus erythematosus; TUNEL, TdT-mediated dUTP-biotin nick end labeling.

<sup>1</sup>Present address of X. Feng: Department of Rheumatology, Affiliated Drum Tower Hospital, Medical School of Nanjing University, Nanjing, China.

<sup>2</sup>To whom correspondence should be addressed.  
e-mail: btsao@mednet.ucla.edu

Manuscript received 4 December 2006 and in revised form 16 January 2007.

Published, JLR Papers in Press, January 26, 2007.  
DOI 10.1194/jlr.M600512-JLR200

fractures compared with a 12% bone fracture frequency in a much older general population in Europe (65–69 years) (7). In addition to age, diabetes, a proinflammatory state, increased cholesterol and estrogen levels, and treatment with corticosteroids also contribute to bone mineral loss in SLE patients (9). Of interest, a recent cross-sectional study revealed an association between disease damage and lower BMD in women with SLE independent of prior use of corticosteroid (10), a finding similar to the described nontraditional risk factor for accelerated atherosclerosis in SLE.

Inflammatory responses to oxidized phospholipids (OxPLs) seem to be shared by atherosclerosis, osteoporosis, and lupus (11, 12). Oxidized low density lipoprotein (OxLDL) has been recognized as a key component in modulating atherosclerosis (13–15). Several OxPLs present in mildly modified/OxLDL, such as 1-palmitoyl-2-(5-oxovaleroyl)-sn-glycero-3-phosphorylcholine (POVPC) and 1-palmitoyl-2-glutaroyl-sn-glycero-3-phosphorylcholine (PGPC), can activate genes necessary for the cellular responses observed in the development of fatty streaks (16). Increased OxLDL (17) and IgG antibodies to OxLDL (17, 18) have been observed in SLE patients compared with normal controls, implying a potential contribution to accelerated atherosclerosis in SLE. Additionally, oxidized lipids can inhibit osteoblastic differentiation and calcium uptake of bone-derived preosteoblasts in vitro (19). Osteoporosis has been observed more frequently in SLE patients with cardiovascular disease, which is also associated with increased OxLDL and autoantibodies to OxLDL (12).

To date, progress in understanding the underlying pathogenesis of atherosclerosis and osteoporosis in SLE has been impaired by the lack of appropriate animal models. Recently, apolipoprotein E-deficient ( $apoE^{-/-}$ ) *gld/gld* (Fas ligand-deficient;  $FasL^{-/-}$ ) C57BL/6 (B6) mice and LDLr.*Sle* mice (radiation chimeras of LDL receptor null B6 mice transplanted with B6.*Sle1.2.3.*) were reported as models of accelerated atherosclerosis (20, 21). These mice develop atherosclerotic lesions, lymphadenopathy, splenomegaly, and autoantibodies on a Western diet. Meanwhile, MRL/lpr mice, which spontaneously develop decreased bone formation and bone turnover compared with age-matched MRL/n mice, are a promising model of osteoporosis in murine lupus (22).

To better understand the link between atherosclerosis, osteopenia, and lupus, we have established a new mouse model, double knockout  $apoE^{-/-}Fas^{-/-}$  B6 mice, which spontaneously develop lupus-like disease, increased atherosclerotic lesions, and decreased BMD by 5 months of age on a normal chow diet. This mouse model is characterized by increased apoptotic cells in renal and heart vessels, decreased levels of OxPL on apoB-100-containing particles, and increased levels of autoantibodies to OxPL in the circulation. Correlations of IgG anti-OxPL levels with atherosclerotic lesions, glomerular tuft areas, and BMD suggest that shared pathways may promote synergy leading to the development of accelerated atherosclerosis, glomerulonephritis, and osteopenia.

## METHODS

### Mice

$apoE^{-/-}$  and  $Fas^{-/-}$  (*lpr/lpr*) mice on the B6 background were purchased from the Jackson Laboratories (Bar Harbor, ME). Single knockout mice were intercrossed and backcrossed to the  $apoE^{-/-}$  parents to produce three groups of mice with the following genotypes:  $apoE^{-/-}Fas^{+/+}$ ,  $apoE^{-/-}Fas^{+/-}$ , and  $apoE^{-/-}Fas^{-/-}$ . DNA was extracted from ear tissue using the Qiagen DNeasy Tissue Kit. Genotyping of the wild-type versus the  $apoE$  knockout allele (23) and the *lpr* allele (24) was performed as described. Mice were fasted for 16 h before bleeding. Serum samples of  $apoE^{-/-}Fas^{+/+}$ ,  $apoE^{-/-}Fas^{+/-}$ , and  $apoE^{-/-}Fas^{-/-}$  littermates at 6 weeks and 5 months of age, and serum samples from  $apoE^{+/+}Fas^{-/-}$  mice at 5 months old, were collected. Mice at 5 or 9 months old were euthanized, with kidneys and heart harvested and spleen weighed. Lumbar vertebrae and limbs were excised. All mice were treated in conformity with Public Health Service policy. They were fed with a regular chow diet and maintained in a temperature-controlled room with a 12 h light/dark cycle according to the approved protocol by the University of California, Los Angeles Animal Research Committee.

### Total IgG and autoantibody detection

Total IgG level was measured with an ELISA kit (Bethyl Laboratories). Serum samples were diluted 1:50 to measure levels of IgG anti-double-stranded DNA (dsDNA) using a streptavidin-biotin method of ELISA (25) and IgG anti-cardiolipin ELISA (26). Serially diluted, pooled serum samples from 43 week old NZB/NZW F1 mice were used to generate standard curves for IgG antibodies to dsDNA or cardiolipin.

Serum IgG and IgM antibodies to POVPC and PGPC were measured with anti-cardiolipin ELISA. Briefly, POVPC or PGPC (Avanti Polar Lipids) at 50  $\mu\text{g}/\text{ml}$  in 100% ethanol was coated onto an Immulon 2 flat plate overnight at 4°C and blocked with 0.25% gelatin/PBS for 1 h at room temperature. After the addition of diluted mouse serum (1:50) samples in duplicate, the plate was incubated for 2 h and developed with the addition of HRP-conjugated goat anti-mouse total IgG or IgM (1:3,000) and tetramethylbenzidine plus hydrogen peroxide as substrate. Serum from one of the  $apoE^{-/-}Fas^{-/-}$  mice with the highest anti-OxPL level was serially diluted to generate standard curves.

### Phenotype of circulating leukocytes

Peripheral blood samples from 5 month old  $apoE^{-/-}$  and  $apoE^{-/-}Fas^{-/-}$  B6 mice were collected to analyze the composition of circulating leukocytes after red-cell lysis and multi-color flow cytometry on a FACSCalibur (BD Biosciences, San Jose, CA) with CellQuest software (BD Biosciences). For the identification of leukocyte subsets, the following markers were used: CD4 and CD8 for T-cells, CD19 for B-cells, NK1.1 for NK-cells, DEC205 for dendritic cells, CD11b+CD16- for neutrophils, and CD11b for monocytes/macrophages. Fluorochrome-conjugated monoclonal antibodies were all purchased from BD PharMingen (San Diego, CA).

### Lipid measurements

Serum lipid levels (total cholesterol, unesterified cholesterol, triglycerides, HDL, and free fatty acids) were measured from 5 month old mice after 16 h of fasting using enzymatic colorimetric assays as described previously (27).

### Serum OxPL detection

The OxPL content of mouse apoB-100-containing lipoprotein particles was assessed using a sandwich chemiluminescence im-

munoassay in which EO6 was used to detect OxPL epitopes on the captured particles and LF5 was used to capture serum apoB-100 (28, 29). Murine apoB-100-specific monoclonal antibodies LF3 and LF5 (30) were purified from the ascites (kindly provided by S. G. Young) using the HiTrap Protein G column (Amersham Biosciences). The protein concentration of the IgG fraction was determined using the Bio-Rad Protein Assay (Bio-Rad). The monoclonal LF5 IgG was biotinylated with EZ-link Sulfo-NHS-Biotin (Pierce) and dialyzed in PBS using Slide-A-Lyzer Dialysis Cassettes (10K MWCO; Pierce).

The apoB-100-specific monoclonal antibody LF3 was coated on FluoroNunc 96-well MaxiSorp plates (Fisher Scientific) at 5  $\mu\text{g/ml}$  in PBS overnight at 4°C. After blocking with 0.25% gelatin-PBS, the plates were incubated with serum (1:80 dilution in PBS) for 1 h at room temperature. Then, biotin-labeled EO6 (2  $\mu\text{g/ml}$  in PBS) was added with biotin-labeled LF5 (2  $\mu\text{g/ml}$  in PBS) in parallel wells to detect the relative amount of apoB captured in each sample for 1 h. The plates were incubated with alkaline phosphatase streptavidin (Vector Laboratories) for 1 h, then incubated with 50% Lumi-Phos (Lumigen, Inc.) in distilled water for 30 min in the dark. The chemiluminescence was read on an Orion Microplate Luminometer (Dynex Technologies), and data were expressed in relative light units (RLU) measured over 100 ms. Each serum sample was measured in duplicate for both EO6 and LF5. The relative number of EO6 epitopes (OxPL) bound per apoB-100 particle was then determined by dividing the bound EO6 RLU by the LF5 RLU.

### Kidney histology and immunofluorescence

Five month old mice were euthanized, and one half of a kidney was fixed in 10% formaldehyde and embedded into paraffin. Three micrometer sections of the kidney tissue were cut and observed for various morphologic lesions after periodic acid Schiff staining. Stained sections were coded and digitally photographed using a microscope fitted with a digital camera (Nikon Eclipse CFI60). Images were analyzed using Image ProPlus software (Media Cybernetics) by a blinded observer to measure the size of the glomerular tuft area as described (31). At least 25 glomeruli per sample were observed in five photographs from different fields of duplicate slides to calculate the mean glomerular tuft area for each mouse.

The other half of the kidney was embedded in Tissue-Tec OCT medium, frozen in liquid nitrogen, and stored at  $-70^{\circ}\text{C}$  until sectioning. Five micrometer frozen sections were fixed with 4% paraformaldehyde and blocked with 2% BSA. Subsequently, slides were stained with fluorescein-conjugated goat anti-mouse IgG (1:150 dilution; Sigma) or fluorescein-conjugated goat IgG fraction to mouse complement C3 (1:150 dilution; Cappel Laboratories), mounted with Gel/Mount (Biomed), and analyzed by fluorescence microscopy. At least 25 glomeruli were observed for each sample.

### Proteinuria measurement

Mice were monitored for proteinuria at  $\sim 1$ –2 months and 5 months of age. Proteinuria was estimated by examination of fresh urine using Albustix (Bayer, Elkhart, IN). Grades of proteinuria were expressed as follows: 0 = none, 1 = trace, 2 =  $\sim 30$  mg/dl, 3 =  $\sim 100$  mg/dl, 4 =  $\sim 300$  mg/ml, and 5 =  $>2,000$  mg/dl.

### Atherosclerotic lesions and heart immunofluorescence

The basal portion of the heart and the proximal aorta were harvested from 5 month old mice, washed in PBS to remove blood, embedded in Tissue-Tec OCT medium, frozen in liquid nitrogen, and stored at  $-70^{\circ}\text{C}$  until sectioning. Serial 10  $\mu\text{m}$

thick cryosections were collected, stained with Oil Red O and hematoxylin and counterstained with fast green, and then examined by light microscopy for the identification of atherosclerotic lesions (32). Methods for IgG and C3 immunofluorescence staining of heart cryosections were the same as those described for kidney immunofluorescence.

### TdT-mediated dUTP-biotin nick end labeling (TUNEL) staining

TUNEL staining of kidney and heart samples was performed according to the manufacturer's protocol (Roche Diagnostics Corp.) with a slight modification. Briefly, cryosections were fixed with 4% paraformaldehyde, permeabilized with freshly prepared 0.2% Triton X-100 in 0.1% sodium citrate on ice, added with the label solution in the presence or absence (negative control) of terminal deoxynucleotidyl transferase, and incubated for 1 h at  $37^{\circ}\text{C}$ . Subsequently, sections were counterstained with 4',6-diamino-phenylindole (1:4,700 dilution; Sigma), and stained images were photographed by fluorescence microscopy. Total cells (stained by 4',6-diamino-phenylindole) and apoptotic cells were counted using Image ProPlus software by a blinded observer.

### BMD determination and three-dimensional microtomography

Excised limbs and vertebrae (including L2–L6 lumbar vertebrae) from 5 or 9 month old female mice were measured for BMD by dual-energy X-ray absorptiometry using a Lunar PIXImus2 instrument (GE Medical Systems, Madison, WI). Limb BMD was the average BMD of both arms and legs. The average value of the left and right femur was calculated as femoral BMD.

Three-dimensional morphometric evaluation of the L5 lumbar vertebra was performed with a microtomographic imaging system ( $\mu\text{CT}$  40; Scanco Medical, Bassersdorf, Switzerland). Parameters determined in the vertebral body included bone volume density (BV/TV), trabecular thickness, trabecular separation, trabecular number, and connectivity density.

### Statistical analysis

The results are presented as means  $\pm$  SEM. Unpaired Student's *t*-test was conducted for comparisons between two groups if the variance was normally distributed, whereas the Mann-Whitney *U* test was used if the variance was not normally distributed. Comparisons among three or more groups were conducted using one-way ANOVA. Correlation between groups was evaluated using the Pearson rank test. Data were calculated using the Prism 3.0 program (GraphPad), and  $P < 0.05$  was considered significant.

## RESULTS

### ApoE<sup>-/-</sup>Fas<sup>-/-</sup> B6 mice display lupus-like autoimmunity

Five month old apoE<sup>-/-</sup>Fas<sup>-/-</sup> B6 mice had significantly enlarged spleens ( $294 \pm 33$  mg;  $n = 16$ ) compared with apoE<sup>-/-</sup>Fas<sup>+/-</sup> ( $98 \pm 9$  mg;  $n = 11$ ) and apoE<sup>-/-</sup>Fas<sup>+/+</sup> ( $72 \pm 6$  mg;  $n = 10$ ) littermates as well as age-matched apoE<sup>+/+</sup>Fas<sup>-/-</sup> mice ( $132 \pm 32$  mg;  $n = 3$ ) ( $P < 0.0001$  by ANOVA). Similarly, apoE<sup>-/-</sup>Fas<sup>-/-</sup> mice had enlarged thymus and lymph nodes. The double knockout mice had significantly reduced levels of circulating CD4<sup>+</sup> and CD8<sup>+</sup> T-cells compared with age-matched apoE<sup>-/-</sup>



Fas<sup>+/+</sup> mice [ $18 \pm 4.5\%$  vs.  $31 \pm 1.3\%$  ( $P = 0.036$ ) and  $17 \pm 1.8\%$  vs.  $22 \pm 0.4\%$  ( $P = 0.024$ ), respectively]. No significant differences in other leukocyte subsets (B-cells, NK-cells, monocytes/macrophages, and neutrophils) were found between 5 month old apoE<sup>-/-</sup>Fas<sup>-/-</sup> and apoE<sup>-/-</sup>Fas<sup>+/+</sup> mice (data not shown).

Serum levels of total IgG and IgG anti-dsDNA were significantly higher in apoE<sup>-/-</sup>Fas<sup>-/-</sup> mice than in apoE<sup>-/-</sup>Fas<sup>+/+</sup> and apoE<sup>-/-</sup>Fas<sup>+/-</sup> littermates at both 6 weeks and 5 months of age (overall  $P < 0.0001$  by ANOVA) (Fig. 1). Compared with 5 month old apoE<sup>+/+</sup>Fas<sup>-/-</sup>

mice, age-matched apoE<sup>-/-</sup>Fas<sup>-/-</sup> mice had increased IgG antibodies to dsDNA ( $P < 0.05$ ). IgG anti-cardiolipin levels were also increased significantly in apoE<sup>-/-</sup>Fas<sup>-/-</sup> mice at 5 months of age compared with those in apoE<sup>+/+</sup>Fas<sup>-/-</sup>, apoE<sup>-/-</sup>Fas<sup>+/+</sup>, and apoE<sup>-/-</sup>Fas<sup>+/-</sup> mice (overall  $P < 0.0001$  by ANOVA).

ApoE<sup>-/-</sup>Fas<sup>-/-</sup> mice exhibited renal damage similar to that found in lupus nephritis patients. Immunofluorescence staining of glomeruli showed that both IgG and C3 were present in the mesangium and peripheral capillary loops of 5 month old apoE<sup>-/-</sup>Fas<sup>-/-</sup> mice (Fig. 2A).

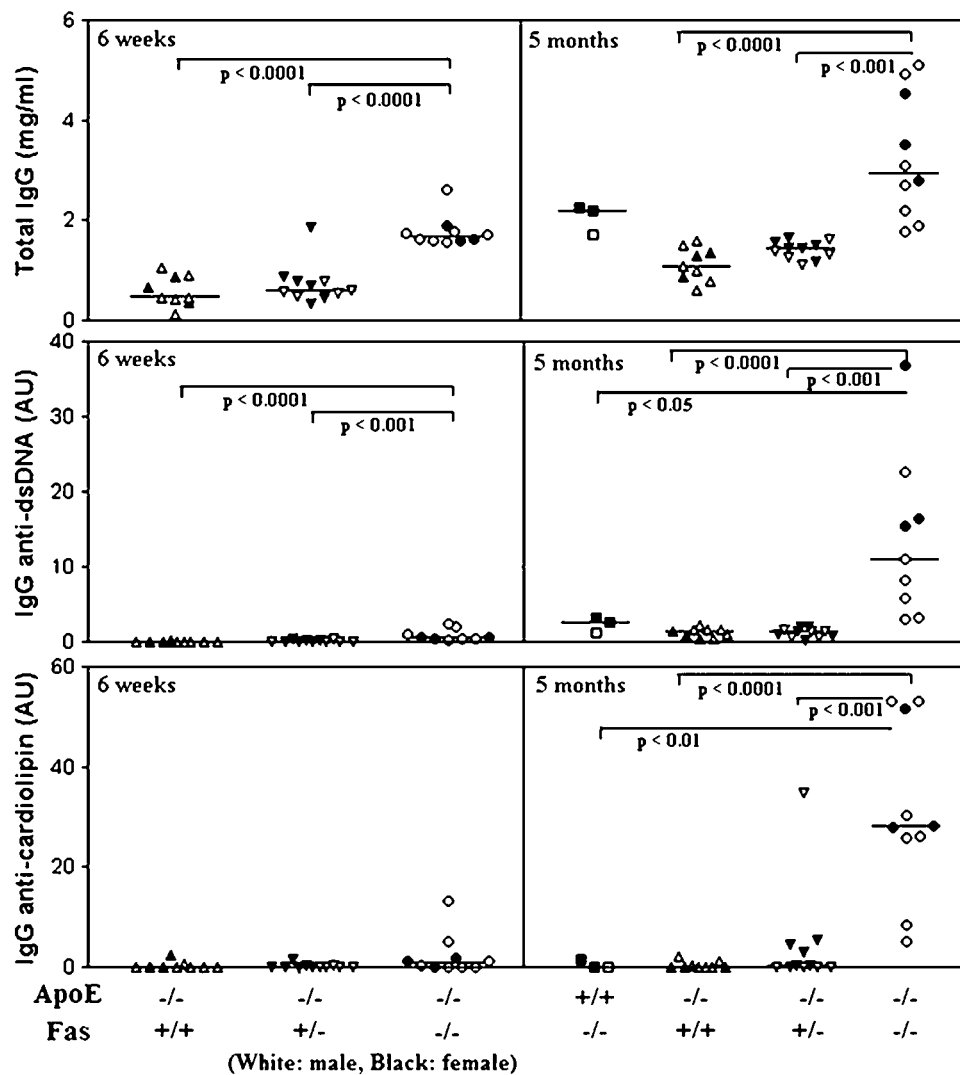


**Fig. 1.** Increased total IgG, IgG anti-double-stranded DNA (dsDNA), and IgG anti-cardiolipin in apolipoprotein E-deficient and Fas<sup>lpr/lpr</sup> (apoE<sup>-/-</sup>Fas<sup>-/-</sup>) C57BL/6 (B6) mice compared with apoE<sup>-/-</sup>Fas<sup>+/-</sup> and apoE<sup>-/-</sup>Fas<sup>+/+</sup> littermates and age-matched apoE<sup>+/+</sup>Fas<sup>-/-</sup> B6 mice. Nine apoE<sup>-/-</sup>Fas<sup>-/-</sup> B6 mice had significantly higher serum IgG and IgG anti-dsDNA levels than their 9 apoE<sup>-/-</sup>Fas<sup>+/+</sup> and 11 apoE<sup>-/-</sup>Fas<sup>+/-</sup> littermates at 6 weeks and 5 months of age (overall  $P < 0.0001$  by ANOVA), whereas increased serum IgG anti-cardiolipin levels in the double knockout mice were evident only at 5 months old (overall  $P < 0.0001$  by ANOVA). Compared with age-matched apoE<sup>+/+</sup>Fas<sup>-/-</sup> mice, 5 month old apoE<sup>-/-</sup>Fas<sup>-/-</sup> mice displayed significantly increased levels of IgG anti-dsDNA ( $P < 0.05$ ) and IgG anti-cardiolipin ( $P < 0.01$ ) but not total IgG. No statistical differences in antibody levels were found between apoE<sup>-/-</sup>Fas<sup>+/+</sup> and apoE<sup>-/-</sup>Fas<sup>+/-</sup> groups. Each symbol represents an individual mouse (white, male; black, female), and lines show median values. Significant  $P$  values of any two-group comparisons are depicted. AU, arbitrary units.

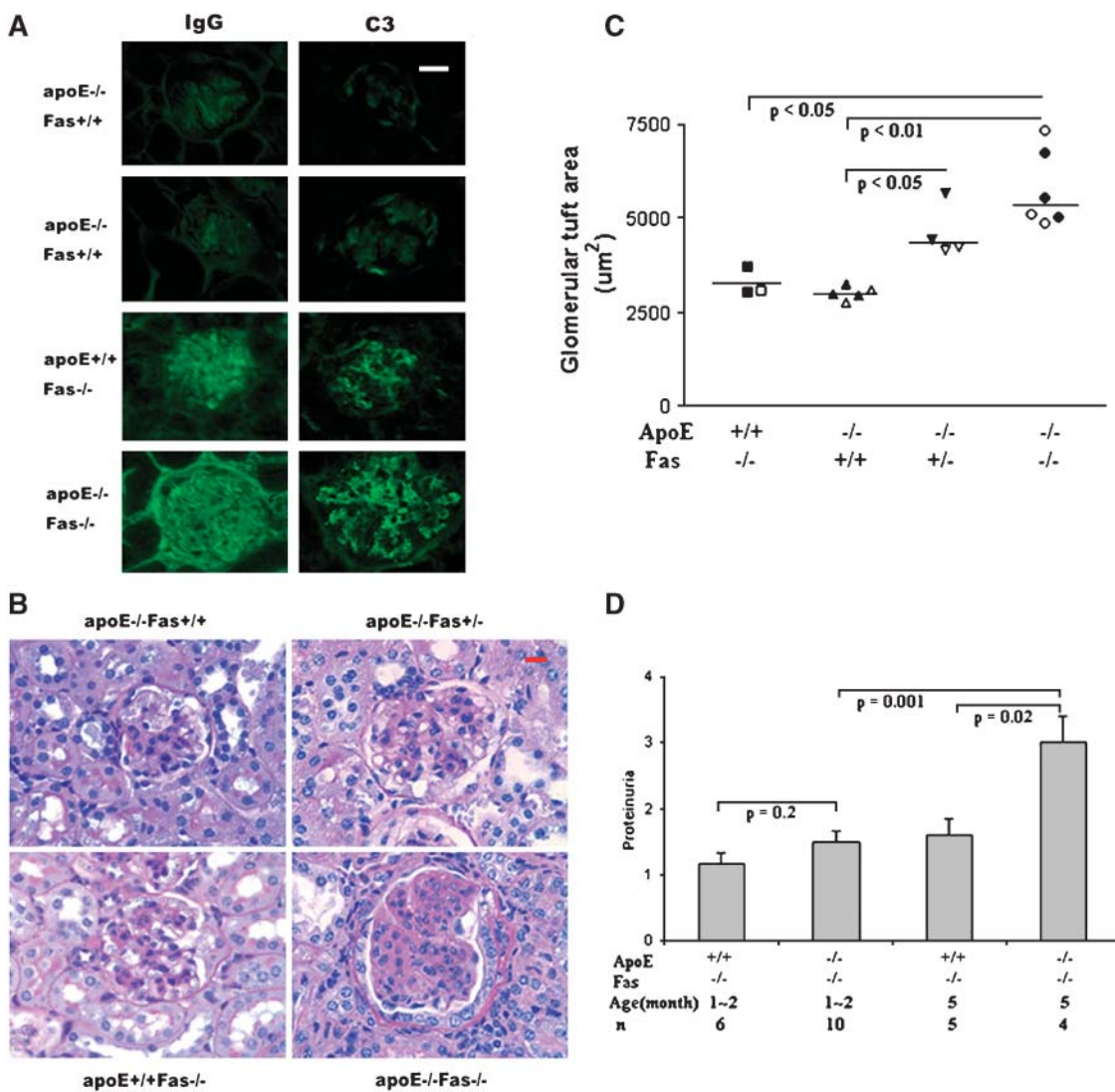


**Fig. 2.** Renal lesions of 5 month old apoE<sup>-/-</sup>Fas<sup>-/-</sup> mice compared with age-matched apoE<sup>-/-</sup>Fas<sup>+/-</sup>, apoE<sup>-/-</sup>Fas<sup>+/+</sup>, and apoE<sup>+/+</sup>Fas<sup>-/-</sup> mice. **A:** Representative photomicrographs of IgG and C3 immunofluorescence in kidney sections (magnification,  $\times 200$ ). A greater amount of IgG and C3 staining of renal sections was found in apoE<sup>-/-</sup>Fas<sup>-/-</sup> mice than in apoE<sup>-/-</sup>Fas<sup>+/-</sup>, apoE<sup>-/-</sup>Fas<sup>+/+</sup>, and apoE<sup>+/+</sup>Fas<sup>-/-</sup> mice, suggesting immune complex-mediated renal injury in apoE<sup>-/-</sup>Fas<sup>-/-</sup> mice. Bar = 20  $\mu\text{m}$ . **B:** The glomerulus of an apoE<sup>-/-</sup>Fas<sup>-/-</sup> mouse was enlarged with hypercellularity and mesangial expansion, displaying characteristic features of glomerulonephritis (periodic acid Schiff staining; magnification,  $\times 600$ ). Bar = 10  $\mu\text{m}$ . **C:** Quantification of glomerular tuft area. Glomerular sizes (means  $\pm$  SEM) in apoE<sup>+/+</sup>Fas<sup>-/-</sup>, apoE<sup>-/-</sup>Fas<sup>+/-</sup>, apoE<sup>-/-</sup>Fas<sup>+/-</sup>, and apoE<sup>-/-</sup>Fas<sup>-/-</sup> mice were 3,409  $\pm$  206  $\mu\text{m}^2$ , 2,988  $\pm$  82  $\mu\text{m}^2$ , 4,629  $\pm$  344  $\mu\text{m}^2$ , and 5,778  $\pm$  394  $\mu\text{m}^2$ , respectively. Each symbol represents an individual mouse, and lines show median values. **D:** Increased proteinuria in apoE<sup>-/-</sup>Fas<sup>-/-</sup> mice. Compared with 5 month old apoE<sup>+/+</sup>Fas<sup>-/-</sup> and  $\sim 1$ -2 month old apoE<sup>-/-</sup>Fas<sup>-/-</sup> mice, 5 month old apoE<sup>-/-</sup>Fas<sup>-/-</sup> mice had increased proteinuria ( $P = 0.018$  vs. 5 month old apoE<sup>+/+</sup>Fas<sup>-/-</sup> mice,  $P = 0.0014$  vs.  $\sim 1$ -2 month old apoE<sup>-/-</sup>Fas<sup>-/-</sup> mice). There was no significant difference between  $\sim 1$ -2 month old and 5 month old apoE<sup>+/+</sup>Fas<sup>-/-</sup> mice. Values shown are means  $\pm$  SEM.

Kidneys from apoE<sup>-/-</sup>Fas<sup>-/-</sup> mice exhibited proliferation of glomerular cells and lobule formation, and mean glomeruli tuft areas of apoE<sup>-/-</sup>Fas<sup>-/-</sup> mice were enlarged compared with those of apoE<sup>-/-</sup>Fas<sup>+/-</sup> and apoE<sup>-/-</sup>Fas<sup>+/+</sup> littermates and age-matched apoE<sup>+/+</sup>Fas<sup>-/-</sup> mice (5,778  $\pm$  394  $\mu\text{m}^2$  vs. 2,988  $\pm$  82  $\mu\text{m}^2$  and 3,409  $\pm$  206  $\mu\text{m}^2$ , respectively;  $P = 0.004$  and  $P = 0.024$ ) (Fig. 2B, C). There were no significant differences in glomeruli tuft areas between male and female mice in each of the four groups. Consistent with the histological

findings, 5 month old apoE<sup>-/-</sup>Fas<sup>-/-</sup> mice had increased proteinuria compared with age-matched apoE<sup>+/+</sup>Fas<sup>-/-</sup> mice (Fig. 2D), which was not evident in younger ( $\sim 1$ -2 month old) mice.

#### ApoE<sup>-/-</sup>Fas<sup>-/-</sup> mice have increased atherosclerotic lesions

The extent of atherosclerotic lesions was measured at the level of aortic valves and in the proximal aorta of each mouse. Measured lesion areas in apoE<sup>-/-</sup>Fas<sup>+/-</sup> mice were

in agreement with values reported previously (27). Neither apoE<sup>-/-</sup>Fas<sup>-/-</sup> nor apoE<sup>-/-</sup>Fas<sup>+/+</sup> mice showed gender differences in their lesion areas. Significantly, increased lesion area was noted at aortic valves in the apoE<sup>-/-</sup>Fas<sup>-/-</sup> mice (n = 11) on normal chow compared with apoE<sup>-/-</sup>Fas<sup>+/+</sup> littermates (n = 16) (0.15 ± 0.012 mm<sup>2</sup> vs. 0.088 ± 0.007 mm<sup>2</sup>, respectively; *P* = 0.0003) (Fig. 3A). In contrast, 5 month old apoE<sup>+/+</sup>Fas<sup>-/-</sup> mice exhibited no evidence for aortic lesions either on a normal chow diet or after a 5 week high-fat diet (data not shown).

Serum total cholesterol and unesterified cholesterol levels of apoE<sup>-/-</sup>Fas<sup>-/-</sup> mice were lower than those of apoE<sup>-/-</sup>Fas<sup>+/+</sup> littermates (*P* < 0.05). No differences in serum triglycerides, HDL cholesterol, or free fatty acids were observed among mice of the three groups (Fig. 3B). The concentrations of HDL and non-HDL cholesterol could not explain the accelerated atherosclerosis in apoE<sup>-/-</sup>Fas<sup>-/-</sup> mice compared with apoE<sup>-/-</sup>Fas<sup>+/+</sup> mice.

Immunofluorescence staining showed IgG deposition in thickened aortic intimas of 5 month old apoE<sup>-/-</sup>Fas<sup>-/-</sup> mice compared with apoE<sup>-/-</sup>Fas<sup>+/+</sup> littermates and age-matched apoE<sup>+/+</sup>Fas<sup>-/-</sup> mice (Fig. 3C). Negligible or trace staining of complement C3 deposition was observed in apoE<sup>-/-</sup>Fas<sup>-/-</sup> mice using immunofluorescence. Increased IgG deposition in the aortic intima and glomerulus support the hypothesis that IgG antibodies and their immune complexes were involved in the development of both atherosclerosis and lupus-like diseases in apoE<sup>-/-</sup>Fas<sup>-/-</sup> mice.

#### Decreased BMD and trabecular bones in female apoE<sup>-/-</sup>Fas<sup>-/-</sup> mice

Dual-energy X-ray absorptiometry analyses showed that BMD of all four limbs from each 5 month old female apoE<sup>-/-</sup>Fas<sup>-/-</sup> mouse was significantly lower than that from male apoE<sup>-/-</sup>Fas<sup>-/-</sup> mice (41.9 ± 0.44 mg/cm<sup>2</sup> vs. 47.1 ± 1.0 mg/cm<sup>2</sup>; *P* = 0.01). Compared with age-matched female apoE<sup>-/-</sup>Fas<sup>+/+</sup> littermates, 5 month old female apoE<sup>-/-</sup>Fas<sup>-/-</sup> mice had decreased femoral BMD (49.6 ± 1.9 mg/cm<sup>2</sup> vs. 55.5 ± 1.5 mg/cm<sup>2</sup>; *P* = 0.040) (Fig. 3D). Vertebrae BMD in apoE<sup>-/-</sup>Fas<sup>-/-</sup> mice also showed a trend of lower levels than in apoE<sup>-/-</sup>Fas<sup>+/+</sup> littermates (52.1 ± 1.7 mg/cm<sup>2</sup> vs. 57.0 ± 1.8 mg/cm<sup>2</sup>; *P* = 0.081). There were no significant differences in femoral and vertebral BMD between apoE<sup>-/-</sup>Fas<sup>-/-</sup> mice and apoE<sup>+/+</sup>Fas<sup>-/-</sup> mice (*P* = 0.37 and *P* = 0.29, respectively). At 9 months old of age, both vertebral and femoral BMD of apoE<sup>-/-</sup>Fas<sup>-/-</sup> mice were significantly lower than those of apoE<sup>-/-</sup>Fas<sup>+/+</sup> littermates (*P* = 0.03 and *P* = 0.02). Three-dimensional morphometric evaluation of the L5 lumbar vertebra in 9 month old mice showed a progressive decrease in trabecular bones of female apoE<sup>-/-</sup>Fas<sup>-/-</sup> mice compared with age-matched female apoE<sup>-/-</sup>Fas<sup>+/+</sup> littermates [BV/TV, 0.092 ± 0.012 vs. 0.17 ± 0.011 (*P* = 0.001); connectivity density (1/mm<sup>3</sup>), 52.4 ± 8.3 vs. 94.2 ± 9.1 (*P* = 0.07); trabecular number (1/mm), 2.6 ± 0.23 vs. 3.2 ± 0.07 (*P* = 0.03); trabecular thickness (mm), 0.046 ± 0.002 vs. 0.053 ± 0.001 (*P* = 0.03)]. The connectivity density of the L5 lumbar vertebra from 9 month old fe-

male apoE<sup>-/-</sup>Fas<sup>-/-</sup> mice was significantly lower than that from apoE<sup>-/-</sup>Fas<sup>+/+</sup> littermates (*P* = 0.03).

#### Increased apoptotic cells in apoE<sup>-/-</sup>Fas<sup>-/-</sup> mice

Renal sections of 5 month old apoE<sup>-/-</sup>Fas<sup>-/-</sup> mice showed an increase in TUNEL-positive fragments compared with those from apoE<sup>-/-</sup>Fas<sup>+/+</sup> and apoE<sup>-/-</sup>Fas<sup>+/-</sup> littermates and aged-matched apoE<sup>+/+</sup>Fas<sup>-/-</sup> mice (Fig. 4A). TUNEL immunofluorescence staining of heart cryosections also showed increased apoptotic cells within the vascular lesions localized predominantly at or near the lumen surface of vessels in apoE<sup>-/-</sup>Fas<sup>-/-</sup> mice (Fig. 4B). The frequency of TUNEL-positive cells, calculated using the number of apoptotic cells divided by the number of total 4',6-diamino-phenylindole-stained cell nuclei in the field (magnification, ×200), was higher in apoE<sup>-/-</sup>Fas<sup>-/-</sup> mice compared with apoE<sup>-/-</sup>Fas<sup>+/+</sup> littermates (median values, 2.43% and 0.12%, respectively; *P* = 0.026) (Fig. 4C). These results, showing increased apoptotic cells in both renal tubules and vessel walls of the heart, suggest that defective apoptosis contributes to disease pathogenesis in apoE<sup>-/-</sup>Fas<sup>-/-</sup> mice.

#### Abnormal serum OxPL and antibodies to OxPL in apoE<sup>-/-</sup>Fas<sup>-/-</sup> mice

Cells undergoing apoptosis generate proinflammatory OxPL on their surfaces and have been shown to be immunogenic (33, 34). Accordingly, we measured circulating levels of OxPL and antibody levels to OxPL in these groups of mice. In 5 month old apoE<sup>-/-</sup>Fas<sup>-/-</sup> mice, the relative amount of serum EO6 epitopes (OxPL) bound per apoB-100 particle was lower than that in 5 month old apoE<sup>-/-</sup>Fas<sup>+/+</sup> and apoE<sup>+/+</sup>Fas<sup>-/-</sup> mice (0.83 ± 0.05 vs. 1.35 ± 0.10 and 1.23 ± 0.09, respectively; *P* < 0.0001 and *P* = 0.0009) (Fig. 5A). IgG anti-POVPC and anti-PGPC antibody levels in these double knockout mice were significantly higher than those in apoE<sup>+/+</sup>Fas<sup>-/-</sup>, apoE<sup>-/-</sup>Fas<sup>+/+</sup>, and apoE<sup>-/-</sup>Fas<sup>+/-</sup> mice at 5 months of age (*P* = 0.012, *P* < 0.0001, and *P* < 0.0007 for IgG anti-POVPC, respectively, and *P* = 0.017, *P* < 0.0001, and *P* < 0.0001 for IgG anti-PGPC, respectively) (Fig. 5B). A trend toward increased levels of IgG anti-POVPC in apoE<sup>-/-</sup>Fas<sup>+/-</sup> mice compared with those in apoE<sup>-/-</sup>Fas<sup>+/+</sup> littermates was also observed (*P* = 0.06). Serum IgM anti-POVPC in apoE<sup>-/-</sup>Fas<sup>-/-</sup> mice was significantly higher than that in apoE<sup>-/-</sup>Fas<sup>+/-</sup> and apoE<sup>-/-</sup>Fas<sup>+/+</sup> mice (*P* < 0.05 and *P* < 0.001, respectively).

As a consequence of increased serum levels of IgG anti-OxPL in apoE<sup>-/-</sup>Fas<sup>-/-</sup> mice, OxPL would be expected to bind to their autoantibodies to form immune complexes that become deposited in tissues. In this study, anti-POVPC and anti-PGPC IgG levels were highly correlated with each other (*r* = 0.95, *P* < 0.0001). Log[anti-POVPC IgG] and log[anti-PGPC IgG] correlated best with glomerular tuft areas (*r* = 0.87, *P* < 0.0001 and *r* = 0.81, *P* = 0.0003, respectively). They also positively correlated with aortic lesion areas and negatively correlated with vertebral BMD and BV/TV (Table 1). These data provide evidence that IgG autoantibodies to these OxPLs are



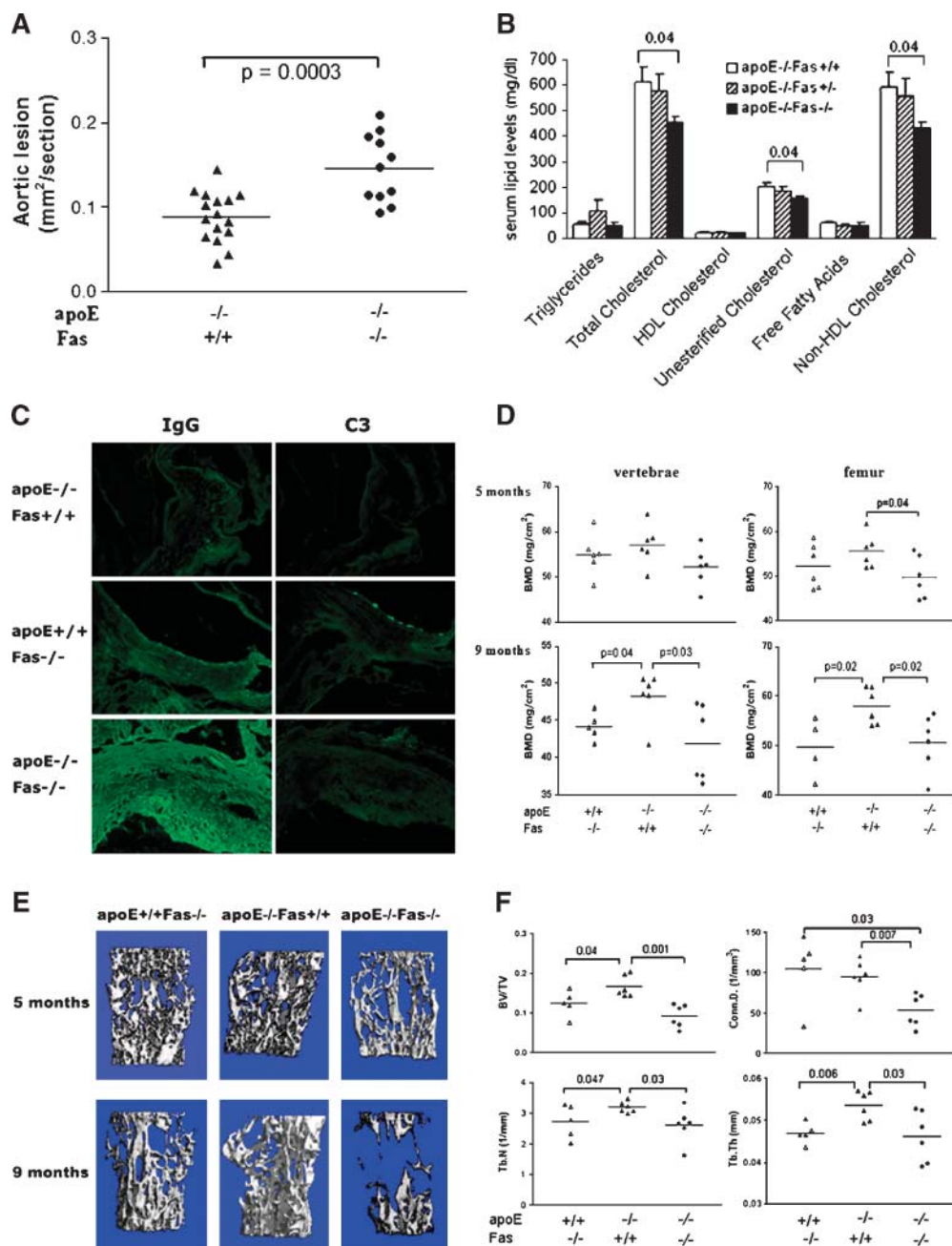


**Fig. 3.** Atherosclerosis and bone loss in apoE<sup>-/-</sup>Fas<sup>-/-</sup> mice. **A:** Larger atherosclerotic lesions were found in 5 month old apoE<sup>-/-</sup>Fas<sup>-/-</sup> mice compared with 5 month old apoE<sup>-/-</sup>Fas<sup>+/+</sup> mice ( $0.15 \pm 0.012 \text{ mm}^2$  vs.  $0.088 \pm 0.007 \text{ mm}^2$ , respectively;  $P = 0.0003$ ). All mice were fed with the normal chow diet and euthanized at 5 months. **B:** Serum total cholesterol, unesterified cholesterol, and non-HDL cholesterol of apoE<sup>-/-</sup>Fas<sup>-/-</sup> B6 mice ( $n = 6$ ) were lower than those of apoE<sup>-/-</sup>Fas<sup>+/+</sup> littermates ( $n = 8$ ). No statistical differences in serum lipid levels were found between apoE<sup>-/-</sup>Fas<sup>+/+</sup> and apoE<sup>-/-</sup>Fas<sup>+/-</sup> groups ( $n = 8$ ). Values shown are means  $\pm$  SEM. **C:** Compared with apoE<sup>-/-</sup>Fas<sup>+/+</sup> and apoE<sup>+/+</sup>Fas<sup>-/-</sup> mice, the aorta vessel intima of apoE<sup>-/-</sup>Fas<sup>-/-</sup> mice had increased IgG staining and trace amounts of staining for complement C3. **D:** Bone mineral density (BMD) of excised vertebrae and femur were measured by dual-energy X-ray absorptiometry. Femoral BMD was calculated as average BMD of left and right femurs, whereas vertebrae BMD was average BMD of L2–L6 lumbar spine sections. The BMD of 5 month old apoE<sup>-/-</sup>Fas<sup>-/-</sup> mice was significantly lower than that of 5 month old apoE<sup>-/-</sup>Fas<sup>+/+</sup> mice ( $P = 0.04$ ). Vertebral BMD of 5 month old apoE<sup>-/-</sup>Fas<sup>-/-</sup> mice showed a trend toward lower levels than that in apoE<sup>-/-</sup>Fas<sup>+/+</sup> mice ( $P = 0.081$ ). There were no significant differences between femoral and vertebrae apoE<sup>-/-</sup>Fas<sup>-/-</sup> mice and apoE<sup>+/+</sup>Fas<sup>-/-</sup> mice ( $P = 0.366$  and  $P = 0.294$ , respectively). At 9 months old of age, both vertebral and femoral BMD of apoE<sup>-/-</sup>Fas<sup>-/-</sup> mice were significantly lower than those of apoE<sup>-/-</sup>Fas<sup>+/+</sup> mice ( $P = 0.03$  and  $P = 0.02$ ). **E:** Representative three-dimensional images of L5 lumbar vertebrae from female mice. Three-dimensional morphometric evaluation of lumbar 5 vertebrae was performed with a microtomographic imaging system ( $\mu$ CT 40; Scanco Medical). The upper panel shows images from 5 month old female mice, and the lower panel shows images from 9 month old female mice. L5 vertebrae from female apoE<sup>-/-</sup>Fas<sup>-/-</sup> mice had less trabecular bone than those from female apoE<sup>-/-</sup>Fas<sup>+/+</sup> and apoE<sup>+/+</sup>Fas<sup>-/-</sup> mice. **F:** Three-dimensional morphometric parameters of lumbar 5 vertebrae from 9 month old female mice. Nine month old female apoE<sup>-/-</sup>Fas<sup>-/-</sup> mice had lower bone volume density (BV/TV;  $P = 0.001$ ), connectivity density (Conn.D.;  $P = 0.007$ ), trabecular number (Tb.N.;  $P = 0.03$ ), and trabecular thickness (Tb.Th.;  $P = 0.03$ ) compared with apoE<sup>-/-</sup>Fas<sup>+/+</sup> mice.

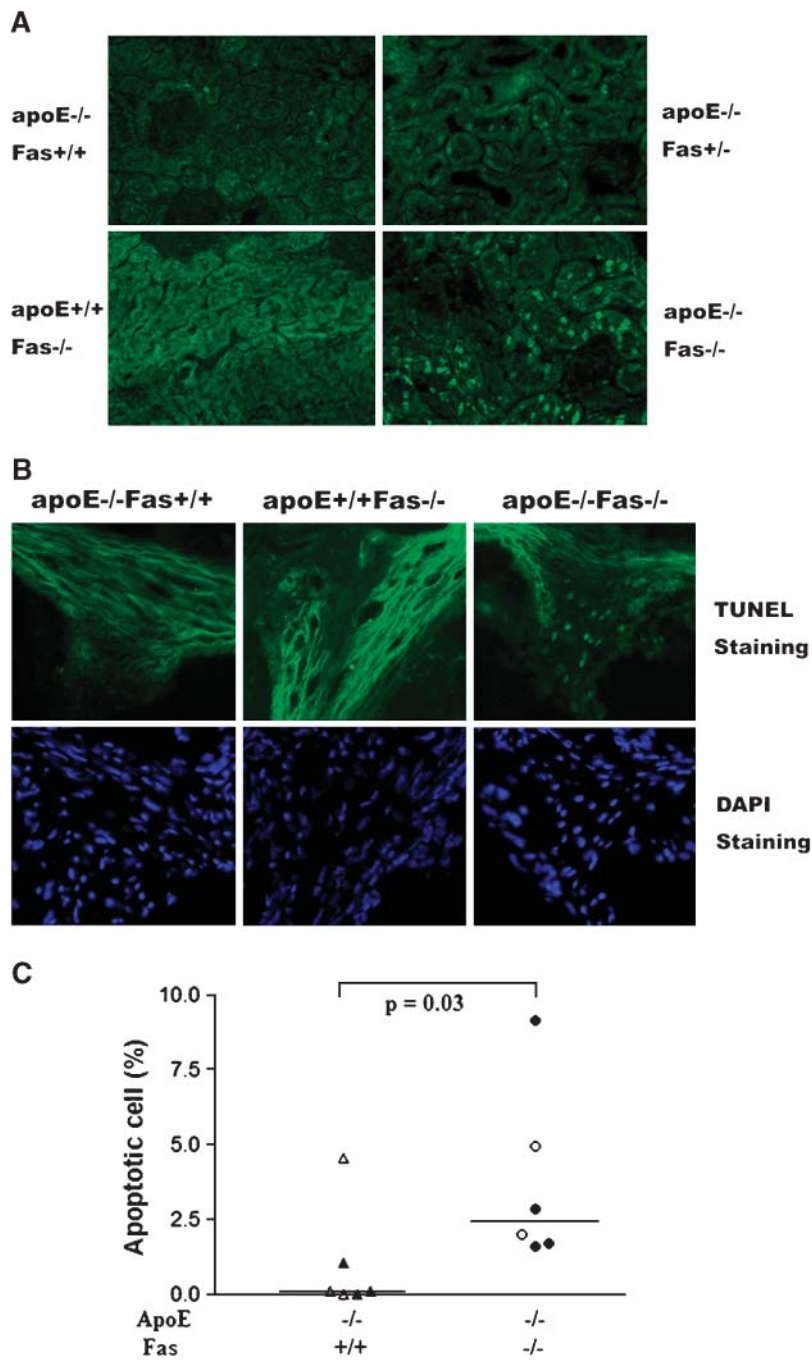


**Fig. 4.** Increased apoptotic signals in 5 month old apoE<sup>-/-</sup>Fas<sup>-/-</sup> mice. **A:** Representative TdT-mediated dUTP-biotin nick end labeling (TUNEL) staining photomicrographs of renal cryosections from 5 month old apoE<sup>-/-</sup>Fas<sup>+/+</sup>, apoE<sup>-/-</sup>Fas<sup>+/-</sup>, apoE<sup>+/+</sup>Fas<sup>-/-</sup>, and apoE<sup>-/-</sup>Fas<sup>-/-</sup> mice. Five micrometer kidney cryosections were used for TUNEL staining. Bright green fluorescein-stained cells marked by the arrow are apoptotic cells (magnification,  $\times 200$ ). A greater amount of TUNEL staining was found in the apoE<sup>-/-</sup>Fas<sup>-/-</sup> mice than in the apoE<sup>-/-</sup>Fas<sup>+/+</sup> and apoE<sup>-/-</sup>Fas<sup>+/-</sup> mice. **B:** Representative TUNEL staining photomicrographs of heart cryosections from 5 month old apoE<sup>-/-</sup>Fas<sup>+/+</sup>, apoE<sup>+/+</sup>Fas<sup>-/-</sup>, and apoE<sup>-/-</sup>Fas<sup>-/-</sup> mice. Ten micrometer heart cryosections were used for TUNEL staining. Apoptotic cells showed bright green color in the photomicrograph (arrow; magnification,  $\times 200$ ). Sections were counterstained with 4',6-diamino-phenylindole (DAPI; staining nuclei blue). Apoptotic debris was mostly localized near the luminal surface of the vessel wall. **C:** TUNEL staining of vessel segments revealed more apoptotic cells within the atherosclerotic lesions of apoE<sup>-/-</sup>Fas<sup>-/-</sup> mice than of apoE<sup>-/-</sup>Fas<sup>+/+</sup> mice. The photomicrographs used were from the fluorescence microscopy shown in B. Subsequently, apoptotic cells and all cells were counted using the Image ProPlus program. Each symbol represents an individual mouse, and lines show median values.  $P = 0.026$  by the Mann-Whitney  $U$  test.



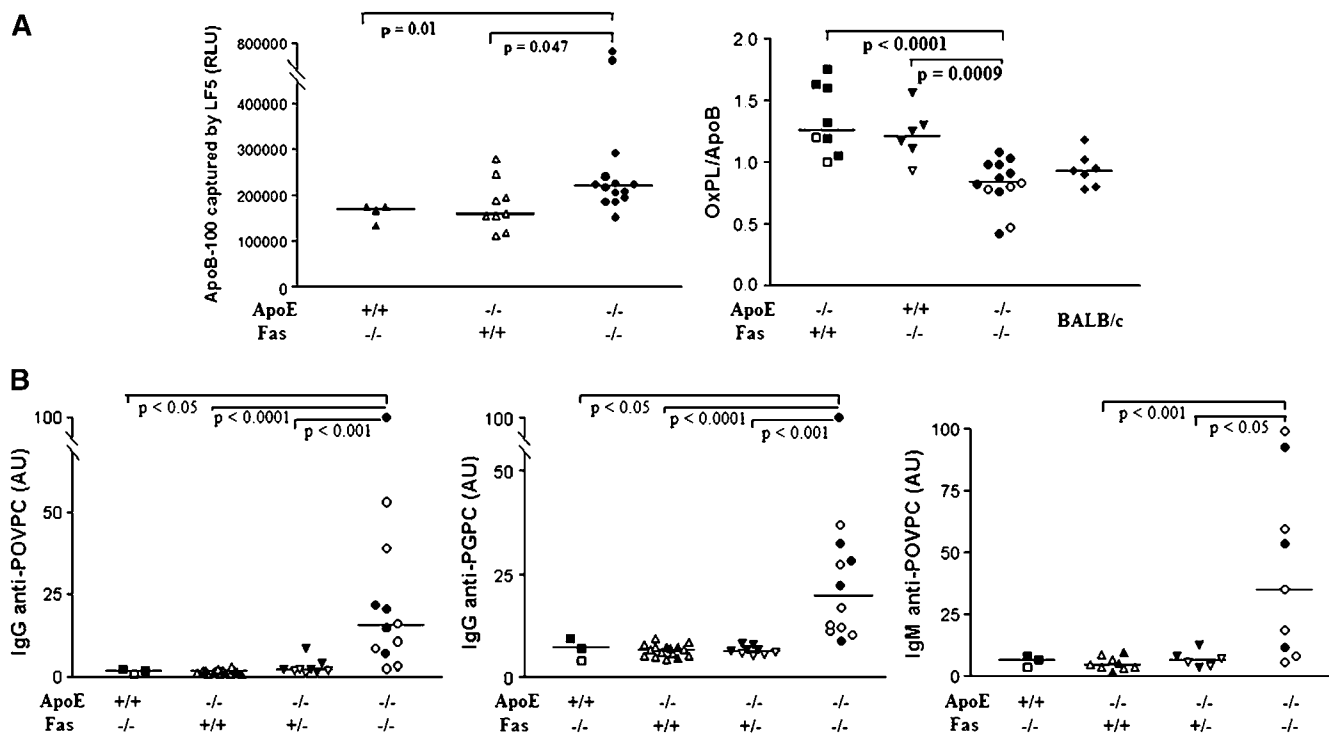


**Fig. 5.** Abnormal serum oxidized phospholipid (OxPL) and IgG antibodies to 1-palmitoyl-2(5-oxovaleroyl)-*sn*-glycero-3-phosphorylcholine (POVPC) and 1-palmitoyl-2-glutaroyl-*sn*-glycero-3-phosphorylcholine (PGPC) in 5 month old apoE<sup>-/-</sup> Fas<sup>-/-</sup> mice. **A:** Serum apoB-100 particles were measured using the murine monoclonal antibodies LF3 and LF5. Data are expressed in relative light units (RLU) measured over 100 ms. Five month old apoE<sup>-/-</sup> Fas<sup>-/-</sup> mice have higher apoB-100 levels than 5 month old apoE<sup>-/-</sup> Fas<sup>+/+</sup> and apoE<sup>+/+</sup> Fas<sup>-/-</sup> mice ( $P = 0.047$  and  $P = 0.01$ , respectively, by the Mann-Whitney  $U$  test). The serum EO6 epitope (OxPL) concentration on apoB-100-containing particles was measured by sandwich chemiluminescence immunoassay. Data are expressed as the ratio EO6/LF5. Five month old apoE<sup>-/-</sup> Fas<sup>-/-</sup> B6 mice have lower EO6/LF5 than 5 month old apoE<sup>-/-</sup> B6 and Fas<sup>-/-</sup> B6 mice ( $0.83 \pm 0.05$  vs.  $1.35 \pm 0.10$  and  $1.23 \pm 0.09$ , respectively;  $P < 0.0001$  and  $P < 0.0009$ ). There was no difference between 5 month old apoE<sup>-/-</sup> Fas<sup>-/-</sup> B6 mice and 6-week-old BALB/c mice. **B:** Serum levels of both IgG anti-POVPC and IgG anti-PGPC were increased in apoE<sup>-/-</sup> Fas<sup>-/-</sup> mice ( $n = 12$ ) compared with age-matched apoE<sup>-/-</sup> Fas<sup>+/+</sup> ( $n = 9$ ), apoE<sup>-/-</sup> Fas<sup>+/+</sup> ( $n = 16$ ), and apoE<sup>+/+</sup> Fas<sup>-/-</sup> ( $n = 3$ ) mice. Serum IgM anti-POVPC in apoE<sup>-/-</sup> Fas<sup>-/-</sup> mice was significantly higher than in apoE<sup>-/-</sup> Fas<sup>+/+</sup> and apoE<sup>-/-</sup> Fas<sup>+/+</sup> mice. AU, arbitrary units.

important contributors to atherosclerosis, osteopenia, and glomerulonephritis.

## DISCUSSION

To our knowledge, the apoE<sup>-/-</sup> Fas<sup>-/-</sup> B6 mouse is the first reported murine model to spontaneously develop

atherosclerosis, osteopenia, and lupus-like disease. Increased apoptosis was shown in aortic and renal sections from apoE<sup>-/-</sup> Fas<sup>-/-</sup> double knockout mice compared with their respective age-matched, single knockout mice. Meanwhile, apoE<sup>-/-</sup> Fas<sup>-/-</sup> mice had a decrease in serum OxPL on apoB-100-containing particles but an increase in serum IgG antibodies to OxPL (POVPC and PGPC). The positive correlation of serum IgG antibodies to OxPL with

**TABLE 1.** Correlations between IgG autoantibodies and glomerular tuft area, aortic lesions, vertebral BMD, and BV/TV

Group	Glomerular Tuft Areas <sup>a</sup> (n = 15)		Aortic Lesions <sup>a,b</sup> (n = 16)		Vertebral BMD <sup>c</sup> (n = 18)		BV/TV <sup>c</sup> (n = 14)	
	r <sup>d</sup>	P	r	P	r	P	r	P
	$\mu\text{m}^2$		$\text{mm}^2/\text{section}$		$\text{mg}/\text{cm}^2$			
Log(anti-dsDNA)	0.65	0.008	0.48	0.06	-0.21	0.47	-0.31	0.28
Log(anti-cardiolipin)	0.69	0.005	0.58	0.02	-0.73	0.003	-0.43	0.13
Log(anti-POVPC)	0.87	<0.0001	0.58	0.02	-0.57	0.03	-0.61	0.02
Log(anti-PGPC)	0.81	0.0003	0.57	0.02	-0.55	0.04	-0.72	0.004

BMD, bone mineral density; BV/TV, bone volume density; dsDNA, double-stranded DNA; PGPC, 1-palmitoyl-2-glutaroyl-*sn*-glycero-3-phosphorylcholine; POVPC, 1-palmitoyl-2(5-oxovaleroyl)-*sn*-glycero-3-phosphorylcholine.

<sup>a</sup>Data from 5 month old mice were used for this calculation.

<sup>b</sup>Data from apolipoprotein E-deficient and Fas<sup>lpr/lpr</sup> (apoE<sup>-/-</sup> Fas<sup>+/+</sup> and apoE<sup>-/-</sup> Fas<sup>-/-</sup>) mice were used for this calculation.

<sup>c</sup>Data from 9 month old female mice were used for this calculation.

<sup>d</sup>Autoantibody levels were transformed to log values, and Pearson  $r$  was calculated.

glomerular tuft areas ( $r > 0.80$ ) and aortic lesion areas ( $r > 0.56$ ) and the negative correlation with vertebrae BMD ( $r < -0.55$ ) and BV/TV ( $r < -0.61$ ) suggest that these autoantibodies and immune complexes may play a role in the pathogenesis of atherosclerosis, glomerulonephritis, and osteopenia.

ApoE and Fas gene deficiencies appear to act synergistically to promote accelerated atherosclerosis and lupus-like disease. Similar to recently reported phenotypes of apoE<sup>-/-</sup>FasL<sup>-/-</sup> B6 mice (20), 5 month old apoE<sup>-/-</sup>Fas<sup>-/-</sup> mice had enlarged spleens, increased IgG antibodies to dsDNA and cardiolipin, increased glomerular deposition of IgG, and enlarged glomerular tuft areas exhibiting features of proliferative glomerulonephritis and proteinuria compared with age-matched apoE<sup>+/+</sup>Fas<sup>-/-</sup> mice (Figs. 1, 2). Consistent with the findings in human SLE (4), accelerated atherosclerosis in our model is independent of lipid-related risk factors, as shown by increased aortic lesions, despite decreased total and non-HDL cholesterol levels in 5 month old apoE<sup>-/-</sup>Fas<sup>-/-</sup> B6 mice compared with apoE<sup>-/-</sup>Fas<sup>+/+</sup> littermates (Fig. 3A, B). Similar results with increased atherosclerosis despite lower levels of pathogenic non-HDL cholesterol and triglycerides were found in LDLr.Sle mice on a Western diet (21). Although levels of HDL and non-HDL cholesterol could not explain the accelerated atherosclerosis in apoE<sup>-/-</sup>Fas<sup>-/-</sup> mice, serum apoB-100 levels were increased in 5 month old apoE<sup>-/-</sup>Fas<sup>-/-</sup> mice compared with age-matched apoE<sup>+/+</sup>Fas<sup>-/-</sup> and apoE<sup>-/-</sup>Fas<sup>+/+</sup> mice (Fig. 5A), suggesting an association between increased apoB-100 levels and accelerated atherosclerosis. ApoB-100 is thought to assemble atherogenic lipoproteins (35), together with increased autoantibody levels, supporting the hypothesis that lipoproteins and immune mechanisms targeting lipoproteins may contribute importantly to increased atherosclerosis. In addition to atherosclerosis and glomerulonephritis, osteopenia is another important complication in SLE that often coexists with atherosclerotic vascular calcification (36). ApoE<sup>-/-</sup> mice have been reported to exhibit enhanced bone formation on a chow diet (37) but decreased bone formation on an atherogenic diet (38). We now show that combined deficiency of both apoE and Fas decreases BMD. In this study, BMD in female apoE<sup>-/-</sup>Fas<sup>-/-</sup> mice was lower than that in age-matched apoE<sup>-/-</sup>Fas<sup>+/+</sup> female mice (Fig. 3D).

In this model, both Fas-mediated apoptosis (39) and apoE-mediated clearance of apoptotic bodies (40) are genetically impaired, which could accelerate the abnormal immune response in apoE<sup>-/-</sup>Fas<sup>-/-</sup> mice. Consistent with observations in gld.apoE<sup>-/-</sup> mice (20), apoE<sup>-/-</sup>Fas<sup>-/-</sup> mice have increased apoptotic cells in the renal and vascular lesions compared with age-matched apoE<sup>-/-</sup>Fas<sup>+/+</sup> and apoE<sup>+/+</sup>Fas<sup>-/-</sup> mice (Fig. 4) (41–44). However, mechanisms connecting impaired apoptosis with target organ damage are still unclear. We have shown previously that syngeneic apoptotic cells are immunogenic in mice and that a surprisingly large number of autoantibodies generated against apoptotic cells are directed toward oxidation-specific epitopes, including OxPL (33,

34, 45). In turn, these OxPLs may form immune complexes with autoantibodies. Adult SLE patients, particularly those with cardiovascular disease, have increased OxPL on LDL and increased IgG and IgM antibodies to OxLDL compared with controls (17). Pediatric SLE patients have increased IgG antibodies to OxLDL and increased IgG immune complexes with LDL, although their levels of oxidized epitopes on LDL are not different from those of controls (18). Similar to SLE patients, serum IgG antibody levels for OxPL (POVPC and PGPC) were increased in apoE<sup>-/-</sup>Fas<sup>-/-</sup> mice compared with the other three groups (Fig. 5B), and increased IgG deposition was found in the thickened aorta intima from 5 month old apoE<sup>-/-</sup>Fas<sup>-/-</sup> mice (Fig. 3C). Interestingly, we found that levels of OxPL on apoB-100-containing particles in 5 month old apoE<sup>-/-</sup>Fas<sup>-/-</sup> mice were lower than in apoE<sup>-/-</sup>Fas<sup>+/+</sup> littermates and age-matched apoE<sup>+/+</sup>Fas<sup>-/-</sup> mice (Fig. 5A). One possibility may be that autoantibodies to OxPL form immune complexes with circulating OxLDL particles, and some of these complexes may be deposited in tissue lesions. SLE patients, particularly those with arterial thrombosis, have increased circulating OxLDL/ $\beta$ 2-glycoprotein I ( $\beta$ 2GPI) complexes (rather than OxLDL/apoB-100 particles) and IgG antibodies to OxLDL/ $\beta$ 2GPI complexes (46), which may be another explanation for the decreased level of serum OxPL in apoE<sup>-/-</sup>Fas<sup>-/-</sup> mice.


Circulating anti-OxPL IgG, but not IgM, may contribute to the development of aortic lesions. Serum IgM anti-POVPC antibody levels were also increased significantly in apoE<sup>-/-</sup>Fas<sup>-/-</sup> mice but showed no correlation with aortic lesion areas (data not shown). In contrast, serum levels of IgG antibodies to OxPL showed strong positive correlation with the extent of lesion areas in the aorta (Table 1). IgG autoantibodies to OxPL have been considered atherogenic (47) and have been correlated with aortic lesion areas in apoE-deficient mice (48, 49), whereas antibodies of the IgM subclass to phosphorylcholine (the head group of POVPC) and OxLDL are protective factors for atherosclerosis (50). Clinical studies have shown that increased IgG titers to OxLDL are related to different manifestations of atherosclerotic disease (reviewed in Ref. 51) and are associated with cardiovascular disease in women affected with SLE (52). Increased serum IgG anti-cardiolipin in our apoE<sup>-/-</sup>Fas<sup>-/-</sup> mice may have a similar role as IgG anti-OxPL antibodies, because many anti-cardiolipin antibodies actually bind to oxidized cardiolipin and may also bind to OxLDL or OxLDL/ $\beta$ 2GPI complexes (44, 46, 53).

Autoantibodies to OxPL are likely to contribute to the severe lupus-like features in apoE<sup>-/-</sup>Fas<sup>-/-</sup> mice. IgG antibodies to dsDNA used to be considered the most important antibody in SLE, especially with glomerulonephritis (54, 55). However, in lupus patients, only 50% of antibodies eluted from glomeruli bound DNA (56). In our model, increased IgG deposition in glomeruli of apoE<sup>-/-</sup>Fas<sup>-/-</sup> mice with increased IgG anti-POVPC and anti-PGPC (Figs. 1A, 5B) suggested that IgG anti-OxPL might act similarly to IgG anti-dsDNA to induce nephritis. Be-

sides, autoantibodies to other oxidation-specific epitopes, such as malondialdehyde, have been suggested to participate in a model of human membrane nephropathy (57).

Moreover, we found that serum levels of IgG autoantibodies to OxPL (POVPC and PGPC), which positively correlated with aortic lesion areas and glomerular tuft areas, correlated negatively with vertebral BMD and bone volume density (Table 1), indicating that IgG anti-OxPL may also be involved in the process of osteoporosis. However, the precise mechanism of osteopenia in this model and the potential role of OxPL and their autoantibodies in bone loss require further investigation.

Factors other than autoantibodies have been shown to play a role in the accelerated atherosclerosis in lupus. In the *gld.apoE<sup>-/-</sup>* murine model on a high-cholesterol Western diet, treatment with simvastatin, the 3-hydroxy-3-methylglutaryl-CoA reductase inhibitor, reduced atherosclerotic lesion area and renal disease and led to reductions in serum tumor necrosis factor- $\alpha$  and IFN- $\gamma$  levels and increases in interleukin-4 and interleukin-10 transcript levels in lymph nodes. These data indicate that a shift from a Th1 to a Th2 cytokine phenotype could ameliorate atherosclerosis and lupus-like autoimmunity (58).

In conclusion, the *apoE<sup>-/-</sup>Fas<sup>-/-</sup>* mouse model is a novel murine model that simultaneously exhibits lupus nephritis, atherosclerosis, and osteopenia. Serum levels of IgG autoantibodies to OxPL (but not anti-dsDNA IgG) correlated negatively with BMD and BV/TV and correlated positively with aortic lesion areas and glomerular tuft areas, suggesting a shared pathway in the pathogenesis of osteopenia, atherosclerosis, and lupus nephritis in these mice. 

This work was supported by a grant from the Lupus Foundation of America (B.P.T.), by National Institutes of Health Grants AR-43814 (B.P.T.) and HL-30568 (A.J.L.), and by a research award from Bristol-Meyer-Squibb (A.J.L.). The authors thank Dr. Richard C. Davis for help in setting up our mouse colony, Dr. Kwan-Ki Hwang for helping us to set up the anti-cardiolipin ELISA, Dr. Ivan Lopez for the use of his fluorescence microscope, Dr. Ram R. Singh for sharing his expertise in setting up renal histology studies, and Dr. Antonio La Cava for critically reviewing the manuscript.

## REFERENCES

- Bacon, P. A., R. J. Stevens, D. M. Carruthers, S. P. Young, and G. D. Kitas. 2002. Accelerated atherogenesis in autoimmune rheumatic diseases. *Autoimmun. Rev.* **1**: 338–347.
- Borchers, A. T., C. L. Keen, Y. Shoenfeld, and M. E. Gershwin. 2004. Surviving the butterfly and the wolf: mortality trends in systemic lupus erythematosus. *Autoimmun. Rev.* **3**: 423–453.
- Roman, M. J., B. A. Shanker, A. Davis, M. D. Lockshin, L. Sammaritano, R. Simantov, M. K. Crow, J. E. Schwartz, S. A. Paget, R. B. Devereux, and D. J. Salmon. 2003. Prevalence and correlates of accelerated atherosclerosis in systemic lupus erythematosus. *N. Engl. J. Med.* **349**: 2399–2406.
- Asanuma, Y., A. Oeser, A. K. Shintani, E. Turner, N. Olsen, S. Fazio, M. F. Linton, P. Raggi, and C. M. Stein. 2003. Premature coronary artery atherosclerosis in systemic lupus erythematosus. *N. Engl. J. Med.* **349**: 2407–2415.
- Manzi, S., E. N. Meilahn, J. E. Rairie, C. G. Conte, T. A. Medsger, Jr., L. Jansen-McWilliams, R. B. Agostino, and L. H. Kuller. 1997. Age-specific incidence rates of myocardial infarction and angina in women with systemic lupus erythematosus: comparison with the Framingham Study. *Am. J. Epidemiol.* **145**: 408–415.
- Esdaille, J. M., M. Abrahamowicz, T. Grodzicky, Y. Li, C. Panaritis, B. R. du, R. Cote, S. A. Grover, P. R. Fortin, A. E. Clarke, and J. L. Senecal. 2001. Traditional Framingham risk factors fail to fully account for accelerated atherosclerosis in systemic lupus erythematosus. *Arthritis Rheum.* **44**: 2331–2337.
- Bultink, I. E., W. F. Lems, P. J. Kostense, B. A. Dijkman, and A. E. Voskuyl. 2005. Prevalence of and risk factors for low bone mineral density and vertebral fractures in patients with systemic lupus erythematosus. *Arthritis Rheum.* **52**: 2044–2050.
- Redlich, K., S. Ziegler, H. P. Kiener, S. Spitzauer, P. Stohlawetz, P. Bernecker, F. Kainberger, S. Grampp, S. Kudlacek, W. Woloszczuk, J. S. Smolen, and P. Pietschmann. 2000. Bone mineral density and biochemical parameters of bone metabolism in female patients with systemic lupus erythematosus. *Ann. Rheum. Dis.* **59**: 308–310.
- Carlsten, H. 2005. Immune responses and bone loss: the estrogen connection. *Immunol. Rev.* **208**: 194–206.
- Lee, C., O. Almagor, D. D. Dunlop, S. Manzi, S. Spies, A. B. Chadha, and R. Ramsey-Goldman. 2006. Disease damage and low bone mineral density: an analysis of women with systemic lupus erythematosus ever and never receiving corticosteroids. *Rheumatology (Oxford)*. **45**: 53–60.
- Demer, L. L. 2002. Vascular calcification and osteoporosis: inflammatory responses to oxidized lipids. *Int. J. Epidemiol.* **31**: 737–741.
- Frostegard, J. 2002. Autoimmunity, oxidized LDL and cardiovascular disease. *Autoimmun. Rev.* **1**: 233–237.
- Binder, C. J., M. K. Chang, P. X. Shaw, Y. I. Miller, K. Hartvigsen, A. Dewan, and J. L. Witztum. 2002. Innate and acquired immunity in atherogenesis. *Nat. Med.* **8**: 1218–1226.
- Frostegard, J. 2005. SLE, atherosclerosis and cardiovascular disease. *J. Intern. Med.* **257**: 485–495.
- Berliner, J. A., and A. D. Watson. 2005. A role for oxidized phospholipids in atherosclerosis. *N. Engl. J. Med.* **353**: 9–11.
- Navab, M., S. Y. Hama, S. T. Reddy, C. J. Ng, B. J. Van Lenten, H. Laks, and A. M. Fogelman. 2002. Oxidized lipids as mediators of coronary heart disease. *Curr. Opin. Lipidol.* **13**: 363–372.
- Frostegard, J., E. Svenungsson, R. H. Wu, I. Gunnarsson, I. E. Lundberg, L. Klareskog, S. Horkko, and J. L. Witztum. 2005. Lipid peroxidation is enhanced in patients with systemic lupus erythematosus and is associated with arterial and renal disease manifestations. *Arthritis Rheum.* **52**: 192–200.
- Soep, J. B., M. Miettus-Snyder, M. J. Malloy, J. L. Witztum, and E. von Scheven. 2004. Assessment of atherosclerotic risk factors and endothelial function in children and young adults with pediatric-onset systemic lupus erythematosus. *Arthritis Rheum.* **51**: 451–457.
- Parhami, F., A. D. Morrow, J. Balucan, N. Leitinger, A. D. Watson, Y. Tintut, J. A. Berliner, and L. L. Demer. 1997. Lipid oxidation products have opposite effects on calcifying vascular cell and bone cell differentiation. A possible explanation for the paradox of arterial calcification in osteoporotic patients. *Arterioscler. Thromb. Vasc. Biol.* **17**: 680–687.
- Aprahamian, T., I. Rifkin, A. Bonegio, B. Hugel, J. M. Freysson, K. Sato, J. J. Castellot, and K. Walsh. 2004. Impaired clearance of apoptotic cells promotes synergy between atherogenesis and autoimmune disease. *J. Exp. Med.* **199**: 1121–1131.
- Stanic, A. K., C. M. Stein, A. C. Morgan, S. Fazio, M. F. Linton, E. K. Wakeland, N. J. Olsen, and A. S. Major. 2006. Immune dysregulation accelerates atherosclerosis and modulates plaque composition in systemic lupus erythematosus. *Proc. Natl. Acad. Sci. USA.* **103**: 7018–7023.
- Schapiro, D., A. Kabala, B. Raz, and E. Israeli. 2001. Osteoporosis in murine systemic lupus erythematosus—a laboratory model. *Lupus.* **10**: 431–438.
- Piedrahita, J. A., S. H. Zhang, J. R. Hagaman, P. M. Oliver, and N. Maeda. 1992. Generation of mice carrying a mutant apolipoprotein E gene inactivated by gene targeting in embryonic stem cells. *Proc. Natl. Acad. Sci. USA.* **89**: 4471–4475.
- Croker, B. P., G. Gilkeson, and L. Morel. 2003. Genetic interactions between susceptibility loci reveal epistatic pathogenic networks in murine lupus. *Genes Immun.* **4**: 575–585.
- Haywood, M. E. K., N. J. Rogers, S. J. Rose, J. Boyle, A. McDermott, J. M. Rankin, V. Thiruudaian, M. R. Lewis, L. Fossati-Jimack, S. Izui, M. J. Walport, and B. J. Morley. 2004. Dissection of BXSB lupus



- phenotype using mice congenic for chromosome 1 demonstrates that separate intervals direct different aspects of disease. *J. Immunol.* **173**: 4277–4285.
26. Edwards, M. H., S. Pierangeli, X. Liu, J. H. Barker, G. Anderson, and E. N. Harris. 1997. Hydroxychloroquine reverses thrombotic properties of antiphospholipid antibodies in mice. *Circulation.* **96**: 4380–4384.
27. Shi, W., X. Wang, N. J. Wang, W. H. McBride, and A. J. Lusis. 2000. Effect of macrophage-derived apolipoprotein E on established atherosclerosis in apolipoprotein E-deficient mice. *Arterioscler. Thromb. Vasc. Biol.* **20**: 2261–2266.
28. Binder, C. J., K. Hartvigsen, M. K. Chang, M. Miller, D. Broide, W. Palinski, L. K. Curtiss, M. Corr, and J. L. Witztum. 2004. IL-5 links adaptive and natural immunity specific for epitopes of oxidized LDL and protects from atherosclerosis. *J. Clin. Invest.* **114**: 427–437.
29. Schneider, M., J. L. Witztum, S. G. Young, E. H. Ludwig, E. R. Miller, S. Tsimikas, L. K. Curtiss, S. M. Marcovina, J. M. Taylor, R. M. Lawn, T. L. Innerarity, and R. E. Pitas. 2005. High-level lipoprotein [a] expression in transgenic mice: evidence for oxidized phospholipids in lipoprotein [a] but not in low density lipoproteins. *J. Lipid Res.* **46**: 769–778.
30. Zlot, C. H., L. M. Flynn, M. M. Veniant, E. Kim, M. Raabe, S. P. A. McCormick, P. Ambroziak, L. M. McEvoy, and S. G. Young. 1999. Generation of monoclonal antibodies specific for mouse apolipoprotein B-100 in apolipoprotein B-48-only mice. *J. Lipid Res.* **40**: 76–84.
31. Muhlfeld, A. S., S. Segerer, K. Hudkins, M. D. Carling, M. Wen, A. G. Farr, J. V. Ravetch, and C. E. Alpers. 2003. Deletion of the fcgamma receptor IIb in thymic stromal lymphopoietin transgenic mice aggravates membranoproliferative glomerulonephritis. *Am. J. Pathol.* **163**: 1127–1136.
32. Qiao, J. H., P. Z. Xie, M. C. Fishbein, J. Kreuzer, T. A. Drake, L. L. Demer, and A. J. Lusis. 1994. Pathology of atheromatous lesions in inbred and genetically-engineered mice—genetic determination of arterial calcification. *Arterioscler. Thromb.* **14**: 1480–1497.
33. Chang, M. K., C. J. Binder, Y. I. Miller, G. Subbanagounder, J. A. Berliner, and J. L. Witztum. 2004. Apoptotic cells with oxidation-specific epitopes are immunogenic and proinflammatory. *J. Exp. Med.* **200**: 1359–1370.
34. Chang, M. K., C. Bergmark, A. Laurila, S. Horkko, K. H. Han, P. Friedman, E. A. Dennis, and J. L. Witztum. 1999. Monoclonal antibodies against oxidized low-density lipoprotein bind to apoptotic cells and inhibit their phagocytosis by elicited macrophages: evidence that oxidation-specific epitopes mediate macrophage recognition. *Proc. Natl. Acad. Sci. USA.* **96**: 6353–6358.
35. Olofsson, S. O., and J. Boren. 2005. Apolipoprotein B: a clinically important apolipoprotein which assembles atherogenic lipoproteins and promotes the development of atherosclerosis. *J. Intern. Med.* **258**: 395–410.
36. Abedin, M., Y. Tintut, and L. L. Demer. 2004. Vascular calcification: mechanisms and clinical ramifications. *Arterioscler. Thromb. Vasc. Biol.* **24**: 1161–1170.
37. Schilling, A. F., T. Schinke, C. Munch, M. Gebauer, A. Niemeier, M. Priemel, T. Streichert, J. M. Rueger, and M. Amling. 2005. Increased bone formation in mice lacking apolipoprotein E. *J. Bone Miner. Res.* **20**: 274–282.
38. Parhami, F., Y. Tintut, W. G. Beamer, N. Gharavi, W. Goodman, and L. L. Demer. 2001. Atherogenic high-fat diet reduces bone mineralization in mice. *J. Bone Miner. Res.* **16**: 182–188.
39. Houston, A., and J. O'Connell. 2004. The Fas signalling pathway and its role in the pathogenesis of cancer. *Curr. Opin. Pharmacol.* **4**: 321–326.
40. Grainger, D. J., J. Reckless, and E. McKilligin. 2004. Apolipoprotein E modulates clearance of apoptotic bodies in vitro and in vivo, resulting in a systemic proinflammatory state in apolipoprotein E-deficient mice. *J. Immunol.* **173**: 6366–6375.
41. Herrmann, M., R. E. Voll, O. M. Zoller, M. Hagenhofer, B. B. Ponner, and J. R. Kalden. 1998. Impaired phagocytosis of apoptotic cell material by monocyte-derived macrophages from patients with systemic lupus erythematosus. *Arthritis Rheum.* **41**: 1241–1250.
42. Perniok, A., F. Wedekind, M. Herrmann, C. Specker, and M. Schneider. 1998. High levels of circulating early apoptotic peripheral blood mononuclear cells in systemic lupus erythematosus. *Lupus.* **7**: 113–118.
43. Ren, Y., J. Tang, M. Y. Mok, A. W. Chan, A. Wu, and C. S. Lau. 2003. Increased apoptotic neutrophils and macrophages and impaired macrophage phagocytic clearance of apoptotic neutrophils in systemic lupus erythematosus. *Arthritis Rheum.* **48**: 2888–2897.
44. Emlen, W., J. Niebur, and R. Kadera. 1994. Accelerated in vitro apoptosis of lymphocytes from patients with systemic lupus erythematosus. *J. Immunol.* **152**: 3685–3692.
45. Huber, J., A. Vales, G. Mitulovic, M. Blumer, R. Schmid, J. L. Witztum, B. R. Binder, and N. Leitinger. 2002. Oxidized membrane vesicles and blebs from apoptotic cells contain biologically active oxidized phospholipids that induce monocyte-endothelial interactions. *Arterioscler. Thromb. Vasc. Biol.* **22**: 101–107.
46. Lopez, L. R., D. F. Simpson, B. L. Hurlley, and E. Matsuura. 2005. OxLDL/ $\beta$ 2GPI complexes and autoantibodies in patients with systemic lupus erythematosus, systemic sclerosis, and antiphospholipid syndrome: pathogenic implications for vascular involvement. *Ann. N. Y. Acad. Sci.* **1051**: 313–322.
47. Matsuura, E., K. Kobayashi, K. Inoue, L. R. Lopez, and Y. Shoenfeld. 2005. Oxidized LDL/ $\beta$ 2-glycoprotein I complexes: new aspects in atherosclerosis. *Lupus.* **14**: 736–741.
48. Pratico, D., R. K. Tangirala, S. Horkko, J. L. Witztum, W. Palinski, and G. A. FitzGerald. 2001. Circulating autoantibodies to oxidized cardiolipin correlate with isoprostane F-2 alpha-VI levels and the extent of atherosclerosis in apoE-deficient mice: modulation by vitamin E. *Blood.* **97**: 459–464.
49. Cyrus, T., D. Pratico, L. Zhao, J. L. Witztum, D. J. Rader, J. Rokach, G. A. FitzGerald, and C. D. Funk. 2001. Absence of 12/15-lipoxygenase expression decreases lipid peroxidation and atherogenesis in apolipoprotein E-deficient mice. *Circulation.* **103**: 2277–2282.
50. Su, J., A. Georgiades, R. Wu, T. Thulin, U. de Faire, and J. Frostegard. 2006. Antibodies of IgM subclass to phosphorylcholine and oxidized LDL are protective factors for atherosclerosis in patients with hypertension. *Atherosclerosis.* **188**: 160–166.
51. Hulthe, J. 2004. Antibodies to oxidized LDL in atherosclerosis development—clinical and animal studies. *Clin. Chim. Acta.* **348**: 1–8.
52. Svenungsson, E., K. Jensen-Urstad, M. Heimburger, A. Silveira, A. Hamsten, U. De Faire, J. L. Witztum, and J. Frostegard. 2001. Risk factors for cardiovascular disease in systemic lupus erythematosus. *Circulation.* **104**: 1887–1893.
53. Horkko, S., T. Olee, L. Mo, D. W. Branch, V. L. Woods, Jr., W. Palinski, P. P. Chen, and J. L. Witztum. 2001. Anticardiolipin antibodies from patients with the antiphospholipid antibody syndrome recognize epitopes in both  $\beta$ (2)-glycoprotein I and oxidized low-density lipoprotein. *Circulation.* **103**: 941–946.
54. Hahn, B. H. 1998. Antibodies to DNA. *N. Engl. J. Med.* **338**: 1359–1368.
55. Ohnishi, K., F. M. Ebling, B. Mitchell, R. R. Singh, B. H. Hahn, and B. P. Tsao. 1994. Comparison of pathogenic and nonpathogenic murine antibodies to DNA—antigen-binding and structural characteristics. *Int. Immunol.* **6**: 817–830.
56. Chowdhry, I. A., C. Kowal, J. Hardin, Z. Zhou, and B. Diamond. 2005. Autoantibodies that bind glomeruli: cross-reactivity with bacterial antigen. *Arthritis Rheum.* **52**: 2403–2410.
57. Neale, T. J., P. P. Ojha, M. Exner, H. Poczewski, B. Ruder, J. L. Witztum, P. Davis, and D. Kerjaschki. 1994. Proteinuria in passive Heymann nephritis is associated with lipid-peroxidation and formation of adducts on type-IV collagen. *J. Clin. Invest.* **94**: 1577–1584.
58. Aprahamian, T., R. Bonaglio, J. Rizzo, H. Perlman, D. J. Lefer, I. R. Rifkin, and K. Walsh. 2006. Simvastatin treatment ameliorates autoimmune disease associated with accelerated atherosclerosis in a murine lupus model. *J. Immunol.* **177**: 3028–3034.